# Evaluation of Silver Exchanged Zeolites Sorbent for the Capture of Radioactive Methyl Iodide

Heong Sub Oh [a] and Jaeyoung Lee [a]
[a]Department of Mechanical and Control Engineering, Handong Univ., Pohang 558, Korea
[*]*Corresponding author: jylee7@handong.edu*

## 1. Introduction

Nuclear energy is powerful, efficient, and reliable. Although it has the deadly problems [1], till it may not be displaced with renewable energy. One of the problems is the emission of volatile radionuclides in the released off-gas stream. [2] High gaseous radioactive chemicals are a direct threat to the peoples and the environment due to high volatile through the atmosphere. [3] Particularly iodine compounds ($^{129}I$ and $^{131}I$) is attended owing to abundant, highly volatile long-lived isotope, which needs to be captured immediately after being released, which seriously affects human metabolic processes. [4] In addition, radioactive iodine is likely form to methyl iodide($CH_3I$), which may not be removed by wet filtering systems.

Porous materials have been developed as sorbents to remove $CH_3I$. Recently various silver zeolites differing by their structure and chemical properties (Si/Al, Ag contents) were investigated for $CH_3I$. Because they include many advantages (removal efficiency, adsorption capacity, thermal stability, cost, and tunable structure). [5] Influence of different parameters on the capture performance of Ag-exchanged zeolites is presented herein, from the oven quartz reactor and GC (gas chromatography) analyzer. Representative results of the evaluations of silver zeolites as sorbent for the dry capture toward $CH_3I$ are presented.

## 2. Materials and methods

Commercial zeolites of structural types sodium ZSM5(16), A, X(Na/X) zeolite (Si/Al = 2.5, 60-80 mesh) were all provided by zeolyst in ammonium or sodium form. Various loadings of silver were introduced into the different zeolitic frameworks by means of ion exchange with silver nitrate (Sigma-Aldrich, purity > 99.8%).

*$CH_3I$ gas-phase dynamic sorption tests:* the adsorption behavior of the silver exchanged zeolites towards volatile $CH_3I$ studied using saturation and breakthrough experiments. The experimental set-up for $CH_3I$ sorption test (Fig.1) can be consisted with three main parts: the generation of the $CH_3I$ inlet concentration, a fixed-bed reactor with controllable temperature (25 ~ 600 ℃) and detection/quantification system composed with a gas chromatography (GC) analyzer equipped with a FID detector. $CH_3I$ adsorption properties of zeolites were tested under air conditions at 50 ~ 250℃ and constant

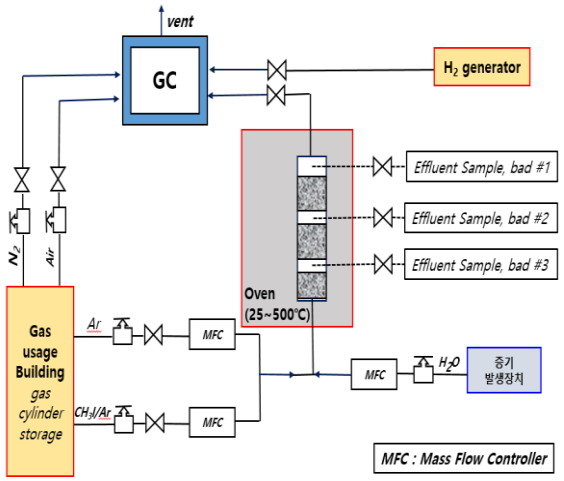


Fig. 1. Experimental set-up used for $CH_3I$ dynamic adsorption tests.

mixed gases flow rate (150ml/min) controlled by mass-flow controller (MFC). Tested sorbents were placed between two parts of quartz wool into a quartz tube loaded itself into a temperature programmed oven.

Prior to adsorption tests, an *in situ* pre-treatment of the samples was performed. The materials were thermally treated into a furnace under argon gas flow. A part of Ar was replaced by $CH_3I$ and the adsorption step was simultaneously started. The initial $CH_3I$ concentration entering the reactor was set to 1000ppm/Ar using a certified $CH_3I$ bottle. The composition at the reactor outflow was continuously monitored using an auto sampler GC analyzer with a FID detector. A typical $CH_3I$ adsorption experiment is shown in the case of Ag/X (2.5) in Fig 2. Adsorption capacities ($Q_{sat}$) at saturation were calculated from integration of $CH_3I$ breakthrough curves using Eq. (1) (see Fig 2, blue zone):

$$Q_{sat} = \frac{D \int_{ti}^{tf} ([CH_3I]_{in} - [CH_3I]_{out}) dt}{m} \qquad \text{Eq. (1)}$$

Where:
- D is the total flow rate (mL/min);
- m is the weight of material (g);
- $[CH_3I]_{in}$: the gas inlet concentration ($ppm_v$);
- $[CH_3I]_{out}$: the gas outlet concentration ($ppm_v$);
- $t_i$: the time corresponding to Ar substitution by $CH_3I$;
- And $t_f$ is the time of bed saturation (min).

## 3. Results and discussion

3.1. Adsorption of $CH_3I$ by the different silver zeolites at T=100 °C.

The prepared sorbent bed submitted to a stream of diluted methyl iodide ([$CH_3I$] =1000 ppm, 150 ml/min). the corresponding breakthrough curves are shown in Fig 2. Table 1. The obtained profiles show some different characteristics such as the time required for breakthrough ($t_{5\%}$ defined by $C/C_0$ = 0.05) and the steepness of $C/C_0$ profiles after breakthrough. Discrimination between the different zeolitic sorbents were assessed quantitatively of adsorption capacities at breakthrough ($Q_{reakthrough}$ at $C/C_0$ = 0.05) and at saturation ($Q_{sat}$) (Fig 2, Table 1).

A typical $CH_3I$ adsorption experiment is shown in the case of Ag zeolites on Fig. 2. Adsorption capacities ($Q_{sat}$) at saturation were calculated from integration of $CH_3I$ breakthrough curves using Eq. (1) (see Figure 2, blue zone): adsorption capacities at bed saturation were used in order to compare performances of different silver zeolites: the protonated ZSM5(16), ammonium form, showed a low adsorption capacity towards $CH_3I$ ($Q_{sat}$ = 35mg/g; Table 1). By contrast, our result data indicate that $CH_3I$ adsorption is improved in presence of silver sites. For the Na/X zeolite containing ca. 15% sodium, a $Q_{sat}$ value of 111mg/g is obtained. In case of Ag/X (2.5) depending on the silver content (from 4.5 to 29.2%), $Q_{sat}$ values between 85 and 179mg/g were obtained. Na/X (2.5). Also, adsorption capacities at breakthrough ($Q_{breakthrough}$) were also quantified through Eq. (1), using $t_{5\%}$ (corresponding to $C/C_0$ = 0.05) instead of $t_f$ (see Fig 2, Table 1).

Our aim was to make a distinction between adsorbed species on the basis of their interaction strength. While maintaining the temperature at 100°C (similar to the adsorption phase), some $CH_3I$ ad-species were removed due to the displacement of the adsorption equilibrium (induced by the substitution of the $CH_3I$/Ar flow) at 100°C. For each Ag zeolites, evacuation was maintained until the $CH_3I$ concentration in the gaseous phase dropped to zero. Weakly-adsorbed species were also quantified (violet zone, Figure 3), in order to give additional insights on the nature of $CH_3I$ trapping (% reversible vs irreversible).

Overall, it can be immediately noticed that the dynamic $CH_3I$ adsorption behavior strongly differs from Ag zeolites to other, showing very different breakthrough times as well as different shapes for the breakthrough profiles. Ag/ZSM-5, Ag/A and Ag/X zeolites displayed classical breakthrough profiles ($Q_{breakthrough}$ and $Q_{sat}$, respectively). ($Q_{breakthrough}$ > 179 mg/g was obtained for Ag/X zeolite with 29 wt% silver at T = 100°C) (Fig. 2 and Table 1).

Possible relationships existing between $CH_3I$ adsorption and the properties of Ag zeolites are discussed. The very low sorption capacity of H-

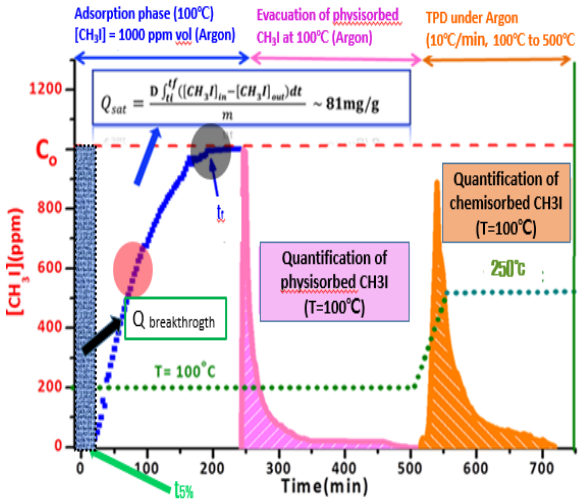


Fig. 2. Typical $CH_3I$ adsorption profile (example of quantification of $Q_{sat}$ and physisorbed $CH_3I$ species for 20Ag/X(2.5).

ZSM5(16) and 5.5Ag ZSM5(16) are easily explained by narrow pore apertures (5-6 Å). Here, our data indicate that the ZSM5(16) is not enough to accommodate $CH_3I$ molecules with a much larger kinetic diameter (estimated value for $CH_3I$: ≈ 5-6 Å [6]). This seems consistent with the low adsorption capacity measured for 5.5Ag ZSM5(16) (Qsat = 51 mg/g). Interestingly, among all the investigated sorbents, Ag/X zeolites with more than 20% silver display the highest adsorption performances thanks to their ion exchange capacities (CEC) (lower Si/Al ratio)

3.2. Quantitative evaluation of trapping stability

Table 1 corresponding to the ability of the different sorbents to promote irreversible trapping as AgI. By contrast with silver zeolites (Fig. 4), the 3.5Ag/ZSM5 (16) and 5.3Ag/A materials with low silver content and small pores enhance the reversible part of trapping at the expense of the irreversible one. The physisorption is

| Sample | $Q_{sat}$ (mg/g) | $Q_{breakthrou}$ (mg/g) | $t_{5\%}$ (min) | $Q_{AgI + NaI}$ |
|---|---|---|---|---|
| *H-ZSM5(16)* | 35 +/- 1 | / | 0 | |
| *5.5AgZSM5* | 51 +/- 2 | 14 +/- 1 | 11+/- 1 | 22 +/- 2 |
| *6.6AgA* | 65 +/- 4 | 17 +/- 2 | 15 +/- 2 | 36 +/- 3 |
| *15.8.NaX(2.5)* | 111 +/- 7 | 22 +/- 3 | 10 +/- 1 | 42 +/- 5 |
| *29.2AgX(2.5)* | 179 +/- 13 | 34 +/- 5 | 20 +/- 5 | 135 +/- 8 |
| *35Ag13X(1.2)* | 253 +/- 12 | 48 +/- 4 | 22 +/- 4 | 180 +/- 9 |

Table 1. $CH_3I$ absorption capacities at breakthrough and saturation at 100°C and silver contents for the different studied silver zeolites.

promoted at the expense of AgI formation. Therefore, such small-pore zeolites are not adequate for long-term $CH_3I$ capture. By contrast, the parent Na/X zeolite displays a significant tendency towards physisorption (39 ± 8 %). Accordingly, the percentage trapped as NaI (14% for 19.3 Na/X) is rather low compared with AgI (60-77% for 29.2 Ag/X zeolite).

## 4. Conclusions

In this study, we have experimentally investigated the performances of Ag exchanged zeolites for the adsorption of gaseous $CH_3I$. Some zeolites structures were selected in order to determine the structural features, which could promote the adsorption of $CH_3I$. Typically, Ag zeolites having pores with a size slightly above the dynamic diameter of $CH_3I$ ($\approx$ 5 - 6Å ) exhibit the best adsorption capacities at 100 ℃. The adsorption of $CH_3I$ of Ag zeolites occurs *via* ab physisorption involving weak (Van der Waals type) bond interactions and another chemisorption involving chemical reaction process. In that respect, desorption data showed that $CH_3I$ retention is a partial reversible at < 250 ℃, with the noticeable different desorption amount of $CH_3I$. Ag/X zeolites with high silver content show the best filtering properties for $CH_3I$ molecules.

Acknowledgments

This work was supported by the Nuclear Safety Research Program through the Korea Foundation Of Nuclear Safety(KoFONS) using the financial resource granted by the Nuclear Safety and Security Commission(NSSC) of the Republic of Korea. (No. 1305008)

## REFERENCES

[1] International Atomic energy Agency, *Nuclear Safety Review*, IAEA/NSR, 2017.
[2] T. H. Woo, *Ann. Nucl. Energy*, 2013, **53**, 197-201.
[3] B. J. Riley, J. D. Vienna, D. M. Strachan, J. S. McCloy and J. L. Jerden, *J. Nucl. Mater*., 2016, **470**, 307-326.
[4] J. R. Goldsmith, C. M. Grossman, W. E. Morton, R. H. Nussbaum, E. A. Kordysh, M. R. Quastel, R. B. Sobel and F. D. Nussbaum, *Environ. Health Perspect*., 1999, **107**, 303-308.
[5] J. Romans and V. Deitz, *Proceedings of the 15th DOE Nuclear Air Cleaning Conference, Conf.* 780819, The Harvard Air Cleaning Laboratory, Cambridge, Massachusetts, 1978, vol. 1.
[6] R.D. Scheele, L.L. Burger, Pacific National Laboratory (1983) PNL.